ORIGINAL PAPER

COMPARISON OF PERFORMANCE PSSs DESIGNED BY NATURE INSPIRED TECHNIQUES AND OPTIMAL CONTROL THEORY

NAVID HORIYAT[1], SEYED MOHAMMAD SHARIATMADAR[2], VAHID AMIR[3]

Manuscript received: 21.01.2014; Accepted paper: 07.03.2014;

Published online: 31.03.2014.

Abstract. *Oscillations of power systems cause instability in power networks; hence PSS is used in conventional methods. Finding suitable gains for PSS is one of the main concerns in designing and determining stability in power networks. Therefore the increase in velocity and the rotor angle can be optimized and compared by using 6^th^ order equations of synchronized machines connected to an infinite network in qdo space and by linearizing the equation in addition to applying genetic optimization, electromagnetic methods, and the theory of optimized control. After analyzing the completed studies, it can be observed that the system will become stable through the use of optimized gains with a higher velocity and a lower rate of error. The mentioned optimized algorithms have been compared with the intent of speeding up system stability.*

Keywords: *Optimized PSS, Riccati method, Stability, Synchronous generator.*

1. INTRODUCTION

The synchronized generator plays a very important role in power networks. Any kind of disorder in the generator causes errors and principle problems in the system. Low frequency causes effects that remain in the system for a long time, affecting operating conditions, sometimes limiting the potential of power transmission. Thus such disturbances affecting the system's capability to maintain synchronism are called small disturbance or small signal [1]. Experiences in power engineering regarding the use of power systems has shown that oscillations are related to the lack of adequate and essential damping in a system's mechanical mode; the appropriate added damping could stabilize a system to an acceptable extent against oscillations. During low frequency oscillations, the induced current in the damping wiring of the generator could be neglected because of its low value. Hence the damping wiring is eliminated in modeling the generator. On the other hand, the normal oscillating frequency of the windings in *"d"*, *"q"* axes of the synchronized rotor is very high, and its specific values will have no particular effects on low frequency oscillations [2-3]. The important role here will be from the machine excitation winding, since its frequency is low and this ending is directly connected to the excitation system, where the complementary controller is applied [4-5]. At this stage the need for a power system stabilizer called *PSS* that

[1] MSc Student of Electrical Power Engineering, Jasb Branch, Islamic Azad University, Jasb, Iran.
E-mail: navid.horiat@gmail.com.
[2] Assistant Professor of Electrical Engineering of Naragh Branch, Islamic Azad University, Naragh, Iran.
E-mail: shariatmadar@iau-naragh.ac.ir.
[3] Kashan Branch, Islamic Azad University, Kashan, Iran. E-mail: v.amir@iaunkashan.ac.ir.

could increase damping by auxiliary stabilizing signals is tangible. At present, power system stabilizers are extensively used in power networks. These stabilizers have acceptable but not optimized performance. Reference [6] in the appendix deals with designing a *PSS* in a machine, connected to an infinite connection by the optimized algorithm of particles compaction. In reference [7], the optimized *PSS* design of a 10-machine system and 39-bus system is made by using simulated annealing (*SA*) and particle swarm optimization (*PSO*) methods in a more optimized way. References [8-9] deal with the optimized design of the *PSS* using the particle swarm optimization method and theory of control method through increasing the speed. In this study the inspired algorithms from the genetic nature and electromagnetism-like method and the theory of optimized control in a synchronized generator connected to an infinite network in speed and rotor angle gains are compared and evaluated, and the obtained results are implemented for the comparisons.

2. DYNAMIC MODEL SYSTEM IN odq FRAME

In this article, a single-machine power system connected to the infinite network has been studied in reference to *"qdo"*. Acceleration and excitation equations in a synchronized generator could be expressed as the dynamics of the synchronized machine, and the equation is stated according to equation 1 [1-3].

$$\begin{aligned} P\Delta\omega_r &= \frac{1}{2H}(T_m - T_e - K_D\Delta\omega_r) \\ P\delta &= \omega_0\Delta\omega_r \\ P\psi_{fd} &= \frac{\omega_0 R_{fd}}{L_{adu}}E_{fd} - \omega_0 R_{fd} i_{fd} \end{aligned} \qquad (1)$$

In these equations, *"P"* is derived operator, "$\omega_0 = 2\pi f_0$" *rad/sec*, "E_{fd}" is the exciter output voltage. The differentiations of the state variables in the equations, however, appear as the functions of "T_e" and "i_{fd}" that should be expressed according to the determined state variables by the flux equations for machine revolution and the network, in reference to *"qdo"*.

3. LINEAR MODEL SYSTEM IN odq FRAME

In analysis and simplification of reference [1-3], the dynamic linearized equations of the machine and the network in reference *"qdo"* are expressed in block diagram as shown in Figure 3. For a better understanding of the system's behavior, the block diagram of Figure 3 is divided into 3 different states in the current study. We will see the first state without considering *AVR* and *PSS* and the second state with the effects of adding *AVR* to the system. In the third state, the system is studied in the final appropriate form, together with *PSS*. Hence the obtained equations are obtained according to the first state and the block diagram in Figure 3 [3].

$$\Delta\dot{\omega}_r = -\frac{K_D}{2H}\Delta\omega_r - \frac{K_1}{2H}\Delta\delta - \frac{K_2}{2H}\Delta\psi_{fd} \qquad (2)$$

$$\Delta\dot{\delta} = \omega_0 \Delta\omega_r$$

$$\Delta\dot{\psi}_{fd} = -\frac{\omega_0 R_{fd}}{L_{fd}} x_1 L'_{ads} \Delta\delta - \frac{\omega_0 R_{fd}}{L_{fd}} [1 - \frac{L'_{ads}}{L_{fd}} + x_2 L'_{ads}] \Delta\psi_{fd}$$

Where the K_1 and K_2 are Constants of the system and also:

$$x_2 = \frac{X_{Tq}}{R_T{}^2 + X_{Tq} X_{Td}} \frac{L_{ads}}{(L_{ads} + L_{fd})}$$
$$R_T = R_a + R_E \qquad (3)$$
$$X_{Tq} = X_E + (L_{aqs} + L_1)$$
$$X_{Td} = X_E + (L_{aqs}{}' + L_1)$$

" Δ_{Tm} " and " ΔE_{fd} " will depend on the drive, and the excitation control devices that are considered to be constants. " L_{aqs} " and " L_{ads} " are the saturated values, and the saturation is shown in small signal studies comprehensively in Reference [3]. Therefore the system simulation results in speed and angular characteristics (values reported at the end of this paper) are according to Fig. 1.

Oscillatory stability state shows the rotor dynamic characteristics in speed and angular gains and increases that primarily increase to maximum values and then reduces. By reducing the state of amplitude, it oscillates to finally obtain its stable state. The above response will have the following aspects in Table 1.

4. SHOWING THE ADDITION OF THYRISTOR EXCITATION SYSTEM WITH AVR

To present and test the stability effect of small signal in the system, a type *ST1A* thyristor excitation model is considered in the 2nd state of the study, as shown in Fig. 2.

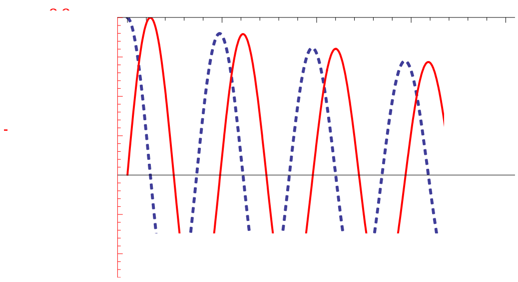

Fig. 1. Response of the System with Speed and Rotor Angle Excitation.

Table 1. Eigenvalues of the System by Stimulating

Parameters	Eigenvalues
$\lambda 1$	-0.2037
$\lambda 2, \lambda 3$	$-0.109568 \pm 6.4177i$

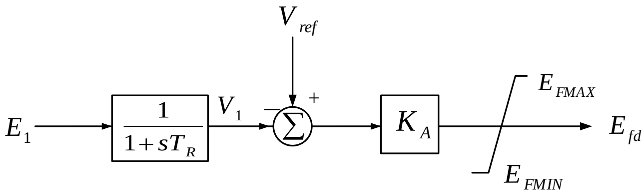

Fig. 2. Thyristor Excitation System with AVR.

Thus the obtained equations are expressed according to the block diagram in Fig. 2 [3, 4]:

$$\Delta\dot{\omega}_r = -\frac{K_D}{2H}\Delta\omega_r - \frac{K_1}{2H}\Delta\delta - \frac{K_2}{2H}\Delta\psi_{fd}$$

$$\Delta\dot{\delta} = \omega_0\Delta\omega_r$$

$$\Delta\dot{\psi}_{fd} = -\frac{\omega_0 R_{fd}}{L_{fd}} x_1 L'_{ads}\Delta\delta - \frac{\omega_0 R_{fd}}{L_{fd}}[1 - \frac{L'_{ads}}{L_{fd}} + x_2 L'_{ads}]\Delta\psi_{fd} - \frac{\omega_0 R_{fd}}{L_{adu}} K_A \Delta v_1 \quad (4)$$

$$\Delta\dot{v}_1 = \frac{K_5}{T_R}\Delta\delta + \frac{K_6}{T_R}\Delta\psi_{fd} + \frac{1}{T_R}\Delta v_1$$

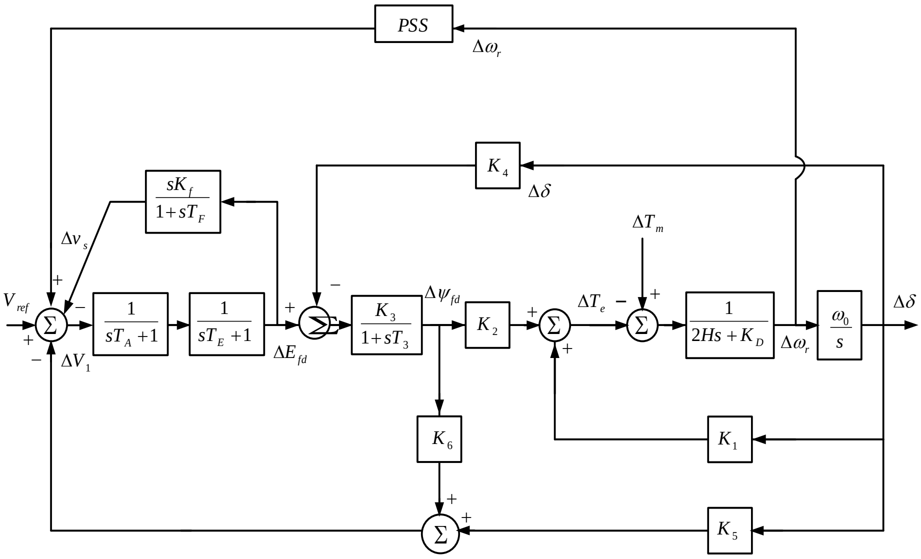

Fig. 3. Small-signal block diagram of the system with Excitation System, AVR and PSS.

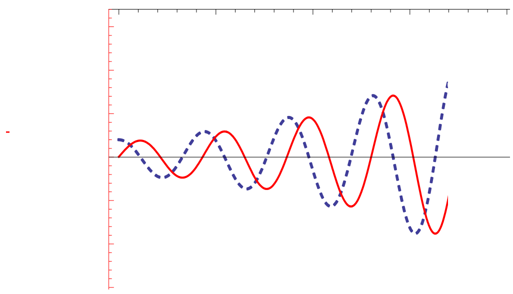

Fig. 4. Response of system with excitation system and AVR.

Table 2. Eigenvalues of the System by Stimulating and AVR

Parameters	Eigenvalues
$\lambda 1$	-31.2294
$\lambda 2$	-20.2025
$\lambda 2, \lambda 3$	$0.504519 \pm 7.23238i$

" Δ_{Tm} " is the mechanical input torque that is considered constant here. "K_6" coefficient is usually assumed positive, while "K_5" could be positive or negative, depending on working conditions and the external network impedance of "Z_{eq}", but it is considered negative in this study, and its effect on the damping torque and synchronizing components is in inverse form (negative damping). Thus the analysis according to the values at the end of this article in speed and angular gains is in the form of the expressed response in Fig. 4 that shows negative damping for the response of the system. This response will have the following aspects in Table 2.

5. ADD OF THE PSS TO THE SYSTEM

We will see the effect of adding PSS to the system in the 3rd state. Relations of the PSS are according to equation 5. The main role of the power stabilizer is to increase the dampness of the system by auxiliary stabilizing signals. The stabilizer should create an electrical torque with a phase similar to rotor speed deviations. Hence one suitable signal for controlling generator excitation is speed deviation shown in block diagram in Fig. 3. Selection of stabilizing parameters to thyristor excitation is described in detail by Reference [3]. Due to the addition of the power system's classical stabilizer, the results are brought in Table 3.

$$
\begin{gathered}
\Delta\dot{\omega}_r = -\frac{K_D}{2H}\Delta\omega_r - \frac{K_1}{2H}\Delta\delta - \frac{K_2}{2H}\Delta\psi_{fd} \\
\Delta\dot{\delta} = \omega_0\Delta\omega_r \\
\Delta\dot{\psi}_{fd} = -\frac{\omega_0 R_{fd}}{L_{fd}}x_1 L'_{ads}\Delta\delta - \frac{\omega_0 R_{fd}}{L_{fd}}[1-\frac{L'_{ads}}{L_{fd}}+x_2 L'_{ads}]\Delta\psi_{fd} - \frac{\omega_0 R_{fd}}{L_{adu}}K_A\Delta v_1 + \frac{\omega_0 R_{fd}}{L_{adu}}K_A\Delta v_s \\
\Delta\dot{v}_1 = \frac{K_5}{T_R}\Delta\delta + \frac{K_6}{T_R}\Delta\psi_{fd} + \frac{1}{T_R}\Delta v_1 \\
\Delta\dot{v}_2 = -K_{STAB}\frac{K_D}{2H}\Delta\omega_r - K_{STAB}\frac{K_1}{2H}\Delta\delta - K_{STAB}\frac{K_2}{2H}\Delta\psi_{fd} - \frac{1}{T_W}\Delta v_2 \\
\Delta\dot{v}_s = -\frac{T_1}{T_2}K_{STAB}\frac{K_D}{2H}\Delta\omega_r - \frac{T_1}{T_2}K_{STAB}\frac{K_1}{2H}\Delta\delta - \frac{T_1}{T_2}K_{STAB}\frac{K_2}{2H}\Delta\psi_{fd} - \frac{T_1}{T_2 T_W} + \frac{1}{T_2}\Delta v_2 - \frac{1}{T_2}\Delta v_s
\end{gathered}
\tag{5}
$$

Table 3. Eigenvalues of the System by Stimulating, AVR And PSS

Parameters	Eigenvalues
$\lambda 1$	-31.4873
$\lambda 2$	-20.4475
$\lambda 3$	-3.45654
$\lambda 4, \lambda 5$	$-1.09516 \pm 6.43661i$
$\lambda 6$	-0.258448

6. DEFINITION OF THE OBJECTIVE FUNCTION

The unstable modes of the system could be identified with this method which takes the males towards stability. Finally, it causes dampness of the responses in rotor speed and angular gains in a shorter time. Thus the equation for system characteristics of which the structure is considered in the system poles could be used. By considering the areas that obtain the above results, the target function could be defined as an overall minimum.

The reason for selecting function minimization is that, if the system poles are located in more negative areas, by considering the limits, that function will be more appropriate. In this paper, select the parameters of the PSS to minimize of objective function are according to equation 6 [4-5]:

$$F = max\{\mathrm{Re}(\lambda_t) + \beta\} \tag{6}$$

where λ_t is closed loop eigenvalue and β is relative stability factor. It is noteworthy that, the efficiency of this target function and its application is in genetic and electromagnetic algorithms.

7. GENETIC ALGORITHM

This algorithm is based on the evolution theory of Darwin. The only part of the population generated in this algorithm is that which has the best characteristics. To determine the optimized parameters of *PSS*, the relevant coefficients are considered chromosomes by using the genetic algorithm. The structure for which is shown in Fig. 5. This algorithm has the same trend as [10].

In this simulation, the number of pairing strings is 20, elite children are 2, and the percentage of produced strings in the interesting method is 80% of the remaining strings. After implementing the genetic algorithm on the linear model of the system, we observed stabilization and the transfer of unstable poles to suitable places, according to Table 4. Furthermore, Table 5 shows the optimal values of PSS parameters obtained by the G-algorithm.

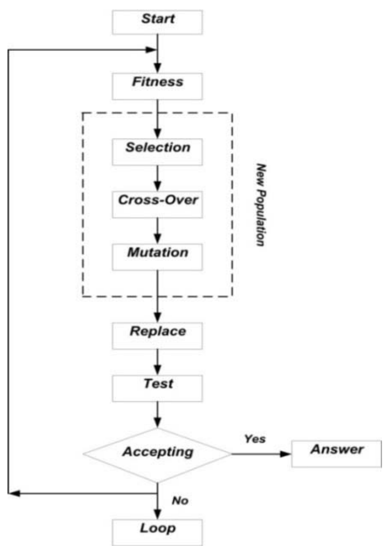

Fig. 5. Structured of Genetic Algorithm.

Table 4. Eigenvalues of Genetic Algorithm.

Parameters	Eigenvalues
$\lambda 1, \lambda 2$	-43.4140
$\lambda 3$	$-15.609 \pm 38.32020i$
$\lambda 4, \lambda 5$	$-0.1644 \pm 2.066011i$
$\lambda 6$	-0.7016

Table 5. Opimized PSS Parameters with GA.

Optimized PSS parameters			
K_{STAB}	$T_1[s]$	$T_2[s]$	$T_W[s]$
9.560	0.13622	0.030	1.40

8. ELECTROMAGNETISM-LIKE ALGORITHM

This algorithm, abbreviated *"EM"*, is known to be one of the new methods in ultra-revelation optimization, based on collective intelligence. One of the strong points of this algorithm is its few parameters, which allows its suitable amount to be determined by trial and error most of the time. In each repeat, the best obtained article in this algorithm is transferred to the next repetition. The procedures and stages of this algorithm can be described in 4 main parts. Hence, the following parameters must be identified and defined before using the algorithm. *"m"* is the number of used particles that is often some 10 digits; *"MaxIter"* is the maximum number of iterations needed to finish the execution of the algorithm, according to Reference [11]; $MaxIter = 25n$; *"n"* is equal to the variables in the case and is clearly dominant in different trial and error problems, on the content of the case; *"LSIter"* is number of local search iterations, and " δ " is the parameter of the local numerical search in [0,1] time.

The general form of the *"EM"* algorithm is expressed as follows:

1: Initialize ()
2: iteration $\leftarrow$ *1*
*3: **while** iteration < MaxIter **do***
4: Local (LSIter , δ *)*
5: ***F*** $\leftarrow$ *CalcF ()*
*6: Move (**F**)*
7: iteration $\leftarrow$ *iteration + 1*
*8: **end While***

The vector of the random response in line 1 is dispersed in the domination of the case. In lines 3 to 8 of the local search procedures " *(Local)"*, calculation of the general force on each of the particles *"(CalcF)"* and displacement of the particles for the imposed force *"(Move)"* is done continually and a definite number of times [11].

8.1. GENERATION OF RANDOM VECTORS

Relation 7 is used to generate random vectors:

$$x_k^i = l_k + \alpha(u_k - l_k) \qquad (7)$$

Where $k = 1,....,n$, $i = 1,...,m$, $\alpha \sim U(0,1)$.

This relation determines the best function value at each point and finds the best place of the vector that leads to the best state for the target function.

8.2. LOCAL SEARCH

After distributing the vectors randomly in the problem domain, the local function deals with the local search adjacent to each response by applying random variations to each component of the vector "x^i".

In this search, the "δ" and "*LSIter*" parameters, respectively, determine the vicinity of the local search. By defining relation 8, we will let the "x^i" components change to the maximum amount.

$$\delta(\max_k \{u_k - l_k\}) \tag{8}$$

Thus each of the "x^i" components will remain in the case of domain. Now, we should temporarily store "x^i" in a variable, such as "y", and then simultaneously change one of the y components randomly and equal to the obtained step in the maximum repetition of "*LSIter*".

If applying the changes leads to a value less than $f(x^i)$ for $f(y)$, then $\{f(y) < f(x^i)\}$ replaces the vector "y" to vector "x^i", and the local search will be performed for the place adjacent to vector "x^{i+1}". After the local search in the neighborhood of all the responding vectors, "x^{best}" will be determined [11].

8.3. CALCULATION OF THE FORCE VECTOR

According to Coulomb's law, the imposed force on each of the two loaded particles in an electrostatic system is equivalent to the multiplication of the load and also equivalent to the inverse square of the distance between two particles.

In the "*EM*" algorithm, as stated, a virtual load is related to each particle, but the relation for the particles varies during the program. Hence after relating a virtual load to each particle, we can calculate total force using a law similar to Coulomb's law. The function "*CalcF*" is used in the general form of the "*EM*" algorithm in line 5 to calculate the imposed force on each virtual particle by other particles in the group. Thus we first relate the virtual load "q^i" to the nth particles in function "*Calc F()*".

The value of "q^i" will be defined according to "x^i" as follows:

$$q^i = \exp\left(-n \frac{f(x^i) - f(x^{best})}{\sum_{k=1}^{m} (f(x^i) - f(x^{best}))} \right) \tag{9}$$

When $i = 1,\ldots,m$, relation 9 shows the optimized related virtual load to each particle. Now to calculate the total imposed force on the i$^{\text{th}}$ particle, "i".e "F^i" that is equal to the total force from other particles on this particle.

It is necessary to calculate the force from jth particles "i".e "F^i" and we use relation 10, [11].

$$F_j^i = \begin{cases} (x^j - x^i) \dfrac{q^i q^j}{\left\| x^j - x^i \right\|^2} & f(x^j) < f(x^i) \\ (x^i - x^j) \dfrac{q^i q^j}{\left\| x^j - x^i \right\|^2} & f(x^i) \le f(x^j) \end{cases} \tag{10}$$

Then in calculating "F^i" we will have:

$$F^i = \sum_{j \neq i}^{m} F_j^i \qquad i = 1,\dots,m \tag{11}$$

The overall results of the above equations show that particles that are less optimized are always observed by the particles with higher optimization states.

8.4. DISPLACEMENT OF THE PARTICLES USING FORSE VECTORS

The function *"Move ()"* in the *"EM"* algorithm expresses the displacement of particles in the case. If the domain is shown by "α" it will be equal to a random variable with homogeneous distribution in time [0,1]. It can be calculated by relation 12:

$$x^i \leftarrow x^i + \alpha \frac{F^i}{\|F^i\|} \vec{R} \tag{12}$$

Where "$\vec{R}$" is a vector defining the permissible limit of variation of each variable. In other words, this vector guarantees that the obtained result 12 is always in the permissible limit$[l_k - u_k]$.

We have chosen the values of parameters "δ" and *"LSIter"* to be 0.01 and 10, respectively. We have also done the simulation by 40 particles and assuming *MaxIter* = 0. Hence after implementing the *"EM"* algorithm on the linear model of the system, we can observe stability and the transfer of unstable poles, according to Table 6. Also, Table 7 shows the optimal values of PSS parameters obtained by the*"EM"* algorithm.

Table 6. Eigenvalues of Electromagnetism-Like Algorithm.

Parameters	Eigenvalues
$\lambda 1, \lambda 2$	-33.609 $\pm$ 5.32020i
$\lambda 3$	-4.1222
$\lambda 4, \lambda 5$	-0.1841 $\pm$ 4.88391i
$\lambda 6$	-0.7014

Table 7. Opimized PSS Parameters with EM.

Optimized PSS parameters			
K_{STAB}	$T_1[s]$	$T_2[s]$	$T_W[s]$
14.2477	0.11710	0. 0377	1.0113

9. OPTIMAL CONTROL THE THEORY

This equation is derived from the optimum linear control of the 2nd method by Liapanov. We will assume in this method that $t \to \infty$ and the starting time is zero. If we want to briefly express this technique in equations 13 to 18, we will have the following [12]:

$$\dot{x}(t) = Ax(t) + Bu(t) \tag{13}$$

Defining the performance index with the aim of minimizing:

$$\int_0^\infty \left[xT(t)Px(t) + x^T(4)Ru(t) \right] dt \tag{14}$$

System input will be the following equation:

$$u(t) = -Kx(t) \tag{15}$$

The matrix stable construction will be:

$$K = R^{-1}B^{T}P \tag{16}$$

"P" in this equation is an undefined symmetrical positive real matrix that is obtained from the following algebraic equation:

$$PA + A^{T}P - PBR^{-1}B^{T}P + Q = 0 \tag{17}$$

And *"Q"* is also a symmetrical real definite matrix.

$$Q = Diag[1,1,1,1,1,1] \tag{18}$$

Hence *R*=1 is considered in this study. It is also assumed that $Q = Diag[10,1,1,1,1,10]$. It is noteworthy that, these parameters are choosen through trial and error. Thus after replacements and required calculations in the mentioned equation, the stabilizing matrix *"K"* will be as relation 19.

$$K = \begin{pmatrix} 28.4130 & 1.0601 & 0.0763 & 0.0099 & 0.7370 & 0.5573 \\ 1.0601 & 0.0844 & 0.0019 & 0.0034 & 0.0503 & 0.0553 \\ 0.0763 & 0.0019 & 0.0589 & 0.0225 & 0.0154 & 0.0264 \\ 0.0099 & 0.0034 & 0.0225 & 0.0223 & 0.0063 & 0.0175 \\ 0.7370 & 0.0503 & 0.0154 & 0.0063 & 1.5144 & 0.1859 \\ 0.5573 & 0.0554 & 0.0264 & 0.0175 & 0.1859 & 0.4957 \end{pmatrix} \tag{19}$$

By applying matrix *"K"* in the $(A - B \cdot K)x(t)$, we can observe the specific values of this process according to Table 8.

Table 8. Eigenvalues of Optimal Control Theory.

Parameters	Eigenvalues
$\lambda 1$	-27.5914
$\lambda 2$	-26.0453
$\lambda 3, \lambda 4$	$-14.1207 \pm 15.8703i$
$\lambda 5$	-7.65115
$\lambda 6$	-1.8995

10. COMPARING THE SIMULATIONS

A comparison of ways to design *PSS* using the optimizing method of genetics, Electromagnetism-Like method, and the optimized control theory has been done in this part. After executing the mentioned algorithms and observing the effects on the responses of speed and angular gains in rotors, we compared the results for previous values as well as after transfer of the specific values according to different working points of the system.

The effect of this analysis in the system's stable or unstable oscillating states is shown in Figs. 6 and 7 demonstrates rotor speed and angular gain for better exhibition and showing optimizing methods.

As can be observed, signal *"a"* in Fig.(6-a) shows the response of the rotor angle with the exciter in the form of Liapanov stability.*"c"* and *"d"* responses are the results from genetic and Electromagnetism-Like ultra-revelation optimization, and it has been seen that the load angle oscillation is improved. The damping speed for response *"b"*, however, since the optimized control method is faster, because it is based on strong mathematics, in optimization, and defines the system optimizing trend. It can also be observed in Fig. (6-b) that the system speed that the response resulting from the optimization theory method causes the system's speed oscillations to be damped faster.

In Figs. (7-a) and (7-b) we can observe the responses of rotor speed and angular gains, despite the existence of the exciter and *AVR*. Response *"a"* shows an oscillating unstable signal. It can be seen that response "b" resulting from the optimized control theory tends faster toward dampness. Hence by defining *"R"* and *"Q"* optimized matrices, the responses will be rather more appropriate and optimized.

Also, the run-time of programs can be compared in Table 9. It is obvious that, the theory of optimal control method uses less run-time than other methods.

Table 9. Comparison of the Run-Time of Programs.

Run-time of programs in Second		
GA	***EM***	***TOCM***
23.4	5.18	1.17

11. CONCLUSIONS

Regards to oscillations that could be occurred in the synchronous machines, the stability of the machine must be kept. Consequently, the machine models must be derived (six order equations in this paper) then the controllers have to use for this purpose. It can be seen that the classic controllers gains finding method (optimal control theory) has best response instead intelligent methods gains finding.

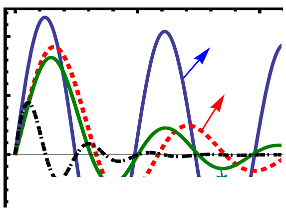

Fig. 6-a. Response of PSSs in Rotor Angle of the Synchronous Generator without AVR.

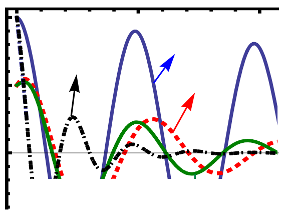

Fig. 6-b. Response of PSSs in Rotor Speed of the Synchronous Generator without AVR.

a : Oscillatory instabilities; b : Riccati PSS; c : GAPSS; d : EMPSS

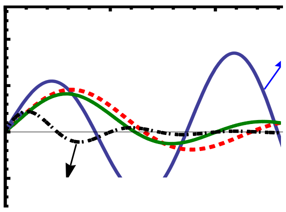

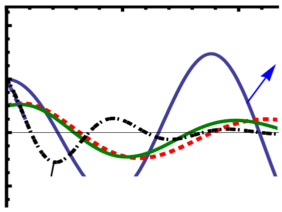

Fig. 7-a. Response of PSSs in Rotor Angle of the Synchronous Generator with AVR.

Fig. 7-b. Response of PSSs in Rotor Speed of the Synchronous Generator with AVR.

a : Oscillatory instabilities; b : Riccati PSS; c : GAPSS; d : EMPSS

APPENDIX

Generator parameters, on the basis unit

$l_{1d} = 0.1713$ $R_{1d} = 0.02840$ $l_{1q} = 0.7252$

$R_{1q} = 0.725$ $R_{1q} = 0.00619$ $l_{2q} = 0.1125$

$l_{adu} = 1.6500$ $l_{aqu} = 1.6000$ $l_1 = 0.16$

$R_a = 0.0030$ $R_{fd} = 0.0006$ $l_{fd} = 0.153$

Parameters of the generator terminal

$p = 0.9$ $Q = 0.436$ $E_t = 1$ $\phi = 25.84^\circ$

Parameters of exciter and stabilizer

K_A=200 K_F=0.026 T_A=0.060s T_E=0.95s T_R=0.02

T_F=1.0s T_W=1 - 20s T_1=0.1 - 1.5s T_2=0.02 - 0.15s

REFERENCES

[1] Yu, Y.N., *Electric power system dynamics*, Academic Press, New York, 2002.

[2] Falehi, A.D., Rostami, M., Doroudi, A., *Turk J Elec Eng & Comp Sci*, **20**, 1010, 2012.

[3] Kundur, P., *Power Systems Stability and Control*, McGraw Hill, New York, 1994.

[4] Abido, M.A., *IEEE Transactions on Energy Conversion*, **15**(3), 297, 2000.

[5] Abido, M.A., Abdel-Magid, Y.L., Mantawy, A.H., *IEEE Transaction on Power Systems*, **15**(2), 735, 2000.

[6] Panda, S., Padhy, N.P., *Int. J.of Electrical and Electronics Engineering*, **1**(1), 1, 2008.

[7] Jeevanandham, A., Thanushkodi, K.G., *Serb.J.of Electrical Engineering*, **6**(1), 89, 2009.

[8] Gui, Sh., Takagi, Y., Ukai, H., *IEEE PowerSystem Technology*, **3**, 1191, 2000.

[9] Babaei, E., Galvani, S., Ahmadi Jirdehi, M., *IEEE Symposium on Industrial Electronics and Applications*, **1**, 325, 2009.

[10] Haupt, R.L., Haupt, S.E., *Practical genetic algorithms*, 2nd edition, Published by John Wiley & Sons, Inc., Hoboken, New Jersey, 2004.

[11] Birbil, S.I., Fang, S.C., *Journal of Global Optimization*, **25**, 263, 2003.

[12] Nazarzadeh, J., Razzaghi, M., Nikravesh, K.Y., *Mathematical and Computer Modelling*, **27**, 51, 1998.